The pion wave function in covariant light-front dynamics

O. Leitner, Jean-Francois Mathiot, N. Tsirova

EPJ manuscript No.
(will be inserted by the editor)

The pion wave function in covariant light-front dynamics

Application to the calculation of various physical observables

O. Leitner[1], J.-F. Mathiot[2], and N. Tsirova[2]

[1] Laboratoire de Physique Nucléaire et de Hautes Énergies, Groupe Théorie, Université Pierre et Marie Curie et Université Diderot, CNRS/IN2P3, 4 place Jussieu, F-75252 Paris, France
[2] Clermont Université, Laboratoire de Physique Corpusculaire, CNRS/IN2P3, BP10448, F-63000 Clermont-Ferrand, France

the date of receipt and acceptance should be inserted later

Abstract. The structure of the pion wave function in the relativistic constituent quark model is investigated in the explicitly covariant formulation of light-front dynamics. We calculate the two relativistic components of the pion wave function in a simple one-gluon exchange model and investigate various physical observables: decay constant, charge radius, electromagnetic and transition form factors. We discuss the influence of the full relativistic structure of the pion wave function for an overall good description of all these observables, including both low and high momentum scales.

PACS. 12.39.Ki Relativistic quark model – 13.40.-f Electromagnetic processes and properties – 14.40.Be Light mesons

1 Introduction

The understanding of the internal structure of hadrons within the standard model is one of the main challenge of nuclear and particle physics. While the high energy limit of the standard model will soon receive new interest from the expected results at LHC, a full nonperturbative description of relativistic bound state systems in Quantum ChromoDynamics (QCD) is still missing. Many theoretical frameworks already exist and shed some light on these systems, like QCD sum rules, lattice QCD or chiral perturbation theory. All of them have their intrinsic theoretical limitations.

In order to have more physical insights into the internal structure of hadrons, we have thus still to rely on constituent quark models. In the sector of up and down quarks, these models should be relativistic. This is also mandatory if one wants to understand physical observables for which the energy scale can be large, like for instance the electromagnetic and transition form factors at high momentum transfer, or the decay constant of the pion. The interest of a phenomenological analysis of the structure of the pion has been renewed by recent experimental data from the Babar collaboration on the pion transition form factor at high momentum transfer [1]. These data (and older ones [2,3]), as well as known data on the pion electromagnetic form factor [4–11] and the precise measurement of the pion decay constant [12] form a rather large set of data to constrain theoretical models in both the low and high momentum domains.

In the very high momentum transfer limit, factorization theorems enable a simple description of exclusive processes like the electromagnetic or transition form factors of the pion in terms of a distribution amplitude [13–18]. This distribution amplitude is an (integrated) amplitude which depends only on the longitudinal momentum fraction of the constituent quark. Corrections from the finite transverse momentum of the constituents may however contribute significantly at low and moderate values of the momentum transfer [19–23]. Moreover, the full structure of the pion involves two spin (or helicity) components [24]. These are a-priori of equal importance in this momentum range.

The first requirement in order to build a relativistic dynamical theory of bound state systems is that it should be invariant under the ten generators of the Poincaré group. These generators include space time translations (four generators), space rotations (three generators) and Lorentz boosts (three generators). Following this requirement, three forms of dynamics have been derived by Dirac already in 1949 [25]. These are the instant form, the point form and the front form.

We shall concentrate in this study on the front form. In this form of dynamics, the system is defined on slices $t^+ = t + z = cte$. This form of dynamics is of particular interest since the boost operator along the z axis is purely kinematical. The electromagnetic form factors are thus particularly simple to calculate. However, the plane $t^+ = cte$ is clearly not invariant under all spatial rotations. The angular momentum operators are therefore dynamical operators. In order to treat in a transparent way the

dependence of these operators on the dynamics, an explicitly covariant formulation of light front dynamics (CLFD) has been derivedin Ref. [26]. The orientation of the light front plane is here characterized by an arbitrary light like four vector ω with $\omega \cdot x = cte$. This approach is a generalization of the standard light-front dynamics (LFD) [27]. The latter can easily be recovered with a special choice of the light-front orientation, $\omega = (1, 0, 0, -1)$.

In the past few years, CLFD has been reviewed [28] and applied to few-body relativistic particle and nuclear physics. This formulation is particularly appropriate to describe hadrons, and all observables related to them, within the constituent quark model. The explicit covariance of this formalism is realized by the invariance of the light-front plane $\omega \cdot x = cte$ under any Lorentz transformation. This implies that ω is not the same in any reference frame, but varies according to Lorentz transformations, like the coordinate x. It is not the case in the standard formulation of LFD where ω is fixed to $\omega = (1, 0, 0, -1)$ in any reference frame. Moreover, the separation of kinematical and dynamical transformations of the state vector provides a definite prescription for constructing bound and scattering states of definite angular momentum. The dynamical dependence of the wave function becomes a dependence on the position of the light-front defined by ω.

As we shall see in this study, this explicitly covariant formalism enables a very simple analysis of the structure of the two-body bound state. The calculation of relativistic corrections, kinematical as well as dynamical, is thus very easy, with a clear connection with non-relativistic approaches since it is also three-dimensional. A similar analysis in the heavy quark sector (structure of the J/Ψ) has already been done in Ref. [29].

In order to constrain the phenomenological structure of hadron wave functions [30–32], one needs to consider several physical observables. In the case of the pion, this includes the decay constant, the electromagnetic form factor and the transition form factor. In our phenomenological study, these observables are calculated in the relativistic impulse approximation. Since our formalism is fully relativistic and can handle the full structure of the pion wave function - in terms of two spin amplitudes - it can describe low as well as high momentum scales, with its full kinematical structure in terms of both the longitudinal momentum fraction and the transverse momentum of the constituent quark and antiquark. This is at variance with most of the previous studies which deal with a single distribution amplitude of the pion [13–18] which may be corrected from transverse momentum contributions [19–23]. A first analysis of the electromagnetic form factor of the pion with the full structure of the pion wave function within the standard formulation of LFD can be found in Ref. [24].

The remainder of this paper is organized as follows. In section 2, we present the basic properties of CLFD. We apply in section 3 our formalism to the pion wave function, and calculate the physical observables in section 4. The numerical results are discussed in section 5. We summarize our results and present our conclusions in section 6.

2 Covariant formulation of light-front dynamics

The description of relativistic systems in CLFD has several nice features particularly convenient in the framework of the relativistic constituent quark model. The most important ones are:

- the formalism does not involve vacuum fluctuation contributions. Therefore, the state vector describing the physical bound state contains a definite number of particles, as given by Fock state components;
- the Fock components of the state vector satisfy a three dimensional equation, and the relativistic wave function has the same interpretation as a probability amplitude, like the non-relativistic one;
- relativistic wave functions and off-shell amplitudes have a dependence on the orientation of the light-front plane which is fully parametrized in terms of the four vector ω. In general, approximate on-shell physical amplitudes also depend on ω, whereas, exact, on-shell physical amplitudes do not depend on the orientation of the light-front plane. This spurious dependence is explicit in CLFD and is therefore under strict theoretical control.

The physical bound state is described by a state vector expressed in terms of Fock components. The state vector is an irreducible representation of the Poincaré group and is fully defined by its mass, M, its four momentum, p, its total angular momentum, J, and the z-axis projection of its angular momentum, λ. The state vector, $|p, \lambda\rangle_\omega$ of the pion of momentum p, defined on a light-front plane characterized by ω (with $\omega \cdot x = 0$ for simplicity), is given in the two-body approximation by [28]

$$|p,\lambda\rangle_\omega = (2\pi)^{3/2} \sum_{\sigma_1,\sigma_2} \int \Phi^{\lambda}_{\sigma_1\sigma_2}(k_1,k_2,p,\omega\tau) \; b^\dagger_{\sigma_1}(\mathbf{k}_1) a^\dagger_{\sigma_2}(\mathbf{k}_2)|0\rangle \delta^{(4)}(k_1+k_2-p-\omega\tau) \; 2(\omega\cdot p)\mathrm{d}\tau \frac{\mathrm{d}^3\mathbf{k}_1}{(2\pi)^{3/2}\sqrt{2\varepsilon_{k_1}}} \frac{\mathrm{d}^3\mathbf{k}_2}{(2\pi)^{3/2}\sqrt{2\varepsilon_{k_2}}} \; , \quad (1)$$

where $\mathbf{k}_i$ is the momentum of the quark (or antiquark) i, of mass m, and $\varepsilon_{k_i} = \sqrt{\mathbf{k}_i^2 + m^2}$. The creation operators for the antiquark and quark are denoted by $b^\dagger$ and $a^\dagger$ respectively; λ is the projection of the total angular momentum of the system on the z axis in the rest frame and σ_i is the spin projections of the particle i in the corresponding rest system. From the delta function, $\delta^{(4)}(k_1 + k_2 - p - \omega\tau)$, ensuring momentum conservation, one gets

$$\mathcal{P} \equiv p + \omega\tau = k_1 + k_2 \; . \quad (2)$$

This peculiar momentum conservation law arises directly from the invariance of the reference system under translations along the light-front time [28]. It is convenient to represent this conservation law in a systematic way. To do that, we shall represent on any diagram the four-vector $\omega\tau$ by a dotted line (the so-called spurion line, see [28] for

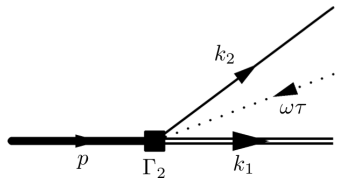

Fig. 1. Representation of the two-body wave function in CLFD. The dotted line represents the off-shell energy of the bound state (spurion), while the thick solid line represents the pion. The quark (antiquark) is shown by a thin solid line (double thin line). The vertex function Γ_2 is defined in Eq. (18).

more details), with an orientation opposite to the quark and antiquark momenta. The two-body wave function Φ will thus be represented by the diagram of Fig. 1. We emphasize that the bound state wave function is always an off-energy shell object ($\tau \neq 0$ due to binding energy) and depends therefore on the light-front orientation. The parameter τ is entirely determined by the on-mass shell condition for the individual constituents, and the conservation law (2). The state vector is normalized according to

$$\langle p', \lambda' | p, \lambda \rangle = 2\varepsilon_p \delta^{(3)}(\mathbf{p} - \mathbf{p}') \delta^{\lambda' \lambda} \ . \tag{3}$$

The two-body wave function $\Phi(k_1, k_2, p, \omega\tau)$ written in Eq. (1) can be parametrized in terms of various sets of kinematical variables. In order to make a close connection to the non-relativistic case, it is more convenient to introduce the following variables [28] defined by

$$\mathbf{k} = L^{-1}(\mathcal{P})\mathbf{k}_1 = \mathbf{k}_1 - \frac{\mathcal{P}}{\sqrt{\mathcal{P}^2}} \left[k_{10} - \frac{\mathbf{k}_1 \cdot \mathcal{P}}{\sqrt{\mathcal{P}^2} + \mathcal{P}_0} \right] \ , \tag{4}$$

$$\mathbf{n} = \frac{L^{-1}(\mathcal{P})\omega}{|L^{-1}(\mathcal{P})\omega|} = \sqrt{\mathcal{P}^2} \frac{L^{-1}(\mathcal{P})\omega}{\omega \cdot p} \ , \tag{5}$$

where $L^{-1}(\mathcal{P})$ is the (inverse) Lorentz boost of momentum $\mathcal{P}$. The momentum $\mathbf{k}$ corresponds, in the frame where $\mathbf{k}_1 + \mathbf{k}_2 = \mathbf{0}$, to the usual relative momentum between the two particles. The unit vector $\mathbf{n}$ corresponds, in this frame, to the spatial direction of ω. Note that this choice of variable does not assume that we restrict ourselves to this particular frame.

The second set of variables which we shall also use in the following is the usual light-front set of coordinates $(x, \mathbf{R}_\perp)$, which is defined by

$$x = \frac{\omega \cdot k_1}{\omega \cdot p} \ ,$$
$$R_1 = k_1 - xp \ ,$$

and where R_1 is decomposed into its spatial components parallel and perpendicular to the direction of the light-front, $R_1 = (R_0, \mathbf{R}_\perp, \mathbf{R}_\parallel)$. We have by definition $R_1 \cdot \omega = 0$, and thus $R_1^2 = -\mathbf{R}_\perp^2$. In the reference frame where $\mathbf{p}_\perp = 0$, $\mathbf{R}_\perp$ is identical to the usual transverse momentum $\mathbf{k}_\perp$. The relations between these two sets of variables are given by

$$\mathbf{R}_\perp^2 \ = \mathbf{k}^2 - (\mathbf{n} \cdot \mathbf{k})^2 \ ,$$
$$x = \tfrac{1}{2} \left[1 - \tfrac{(\mathbf{n} \cdot \mathbf{k})}{\epsilon_k} \right] \ . \tag{6}$$

The inverse relations read:

$$\mathbf{k}^2 = \frac{\mathbf{R}_\perp^2 + m^2}{4x(1-x)} - m^2 \ ,$$
$$\mathbf{n} \cdot \mathbf{k} = \left[\frac{\mathbf{R}_\perp^2 + m^2}{x(1-x)} \right]^{1/2} \left(\frac{1}{2} - x \right) \ . \tag{7}$$

Note that $\mathbf{k}^2$ and $\mathbf{n} \cdot \mathbf{k}$ are invariant under any rotation and Lorentz boost [28], like x and $\mathbf{R}_\perp^2$. In the non relativistic limit, $\mathbf{n} \equiv \mathbf{n}/c \to 0$ and therefore $x \to 1/2$ and $\mathbf{n}.\mathbf{k} \to 0$.

3 The pion wave function

3.1 Structure of the bound state

The covariance of our approach allows to write down explicitly the general spin structure of the two-body bound state. For a pseudoscalar particle of momentum p, composed of an antiquark and a quark of equal masses m and of momenta k_1 and k_2, respectively, it takes the form

$$\Phi^{\lambda=0}_{\sigma_1 \sigma_2} = \frac{1}{\sqrt{2}} \bar{u}_{\sigma_2}(k_2) \left(A_1 \frac{1}{m} + A_2 \frac{\not{\omega}}{\omega \cdot p} \right) \gamma_5 \ v_{\sigma_1}(k_1) \ , \tag{8}$$

where $v(k_1)$ and $u(k_2)$ are the usual Dirac spinors, and A_1 and A_2 are the two scalar components of the pion wave function. For simplicity, we shall also call wave functions these two spin components. They depend on two scalar variables, which we shall choose as $(x, \mathbf{R}_\perp^2)$. We do not show for simplicity the standard isospin and color components of the pion wave function in Eq. (8). The representation of this wave function in terms of the variables $\mathbf{k}$ and $\mathbf{n}$ is given by

$$\Phi^0_{\sigma_1 \sigma_2} = \frac{1}{\sqrt{2}} w^t_{\sigma_2} \left(g_1 + \frac{i\sigma \cdot [\mathbf{n} \times \mathbf{k}]}{k} g_2 \right) w_{\sigma_1} \ , \tag{9}$$

where w_i are Pauli spinors and $g_{1,2}$ are the two scalar components of the pion wave function in this representation. They depend also on two scalar variables, which we shall choose as $(\mathbf{k}^2, \mathbf{k}.\mathbf{n})$. One can easily express $A_{1,2}$ in terms of $g_{1,2}$. We get [1]

$$g_1 = \frac{2\varepsilon_k}{m} A_1 + \frac{m}{\varepsilon_k} A_2 \ , \tag{10}$$

$$g_2 = -\frac{k}{\varepsilon_k} A_2 \ . \tag{11}$$

[1] One uses here the standard definition of γ^5 with positive sign for its matrix elements, contrarily to [28] where γ^5 has an opposite sign.

We would like to stress that the decomposition (8) is a very general one for a spin zero particle composed of two spin 1/2 constituents. In the non-relativistic limit, the component $g_1(\mathbf{k}^2, \mathbf{k}.\mathbf{n})$ only survives and depends on a single scalar variable $\mathbf{k}^2$. In our phenomenological analysis, we shall therefore start from a non-relativistic component, g_1^0, given by a simple parametrization. We shall use in the following either a gaussian wave function given by

$$g_1^0(\mathbf{k}^2) = \alpha \, \exp(-\beta \, \mathbf{k^2}) \; , \tag{12}$$

or a power-law wave function written as

$$g_1^0(\mathbf{k}^2) = \frac{\alpha}{(1+\beta \, \mathbf{k^2})^\gamma} \; , \tag{13}$$

where β is a parameter to be determined from experimental data, while α will be fixed from the normalization condition. The power γ will be chosen equal to 2. The relativistic component A_2, as well as dynamical relativistic corrections to A_1, will be calculated from radiative corrections, as explained in the next subsection. The choice (12) is equivalent to the Brodsky-Huang-Lepage parametrization [33].

The normalization condition writes [28]

$$1 = \sum_{\sigma_1 \sigma_2} \int dD \; \Phi^\lambda_{\sigma_1\sigma_2} \Phi^{\lambda\star}_{\sigma_1\sigma_2} \; , \tag{14}$$

where dD is an invariant phase space element which can take the following forms, depending on the kinematical variables which are used

$$dD = \frac{1}{(2\pi)^3} \frac{\mathrm{d}^3\mathbf{k}_1}{(1-x)2\varepsilon_{k_1}} = \frac{1}{(2\pi)^3} \frac{\mathrm{d}^3\mathbf{k}}{2\varepsilon_k} = \frac{1}{(2\pi)^3} \frac{\mathrm{d}^2\mathbf{R}_\perp \mathrm{d}x}{2x(1-x)} \; . \tag{15}$$

With the pion wave function written in Eq. (8), the normalization condition writes [28]

$$1 = \frac{1}{(2\pi)^3} \int \frac{\mathrm{d}^2\mathbf{R}_\perp \mathrm{d}x}{2x(1-x)} \left[\frac{\mathbf{R}_\perp^2 + m^2}{m^2 x(1-x)} A_1^2 + 4A_1A_2 + 4x(1-x)A_2^2 \right] . \tag{16}$$

3.2 Radiative corrections to the wave function

In a traditional non-relativistic study of the pion wave function in the spirit of the constituent quark model, one may start directly from a simple parametrization of the component g_1^0, as given for instance in Eqs. (12,13). However, it is necessary to correct this wave function in some way in order to incorporate in a full relativistic framework the high momentum tail given by the one-gluon exchange mechanism. We shall achieve this using perturbation theory, starting from the zeroth order wave function g_1^0.

The (eigenvalue) equation we start from to calculate the bound state wave function is represented schematically in Fig. 2. According to the diagrammatic rules of CLFD, this equation writes, in the case of spin 1/2 particles [28]

$$\bar{u}(k_2) \Gamma_2 v(k_1) = \int \frac{\mathrm{d}^3\mathbf{k_1}}{2\varepsilon_{k_1}(2\pi)^3} \frac{\mathrm{d}\tau'}{\tau' - i\epsilon} \delta(k_2'^2 - m^2) \Theta(\omega{\cdot}k_2') \times \bar{u}(k_2) \left[\gamma_\mu (\not{k}_2' + m) \Gamma_2'(m - \not{k}_1')\gamma_\nu\right] K^{\mu\nu} v(k_1) \; . \tag{17}$$

It is written in terms of the two-body vertex function Γ_2 defined by [34]

$$\bar{u}(k_2) \Gamma_2 v(k_1) \equiv (s - M_\pi^2) \Phi \; , \tag{18}$$

with

$$s = \frac{\mathbf{R}_\perp^2 + m^2}{x} + \frac{\mathbf{R}_\perp^2 + m^2}{(1-x)} \; . \tag{19}$$

The mass of the pion is denoted by M_π. We shall define for simplicity

$$\mathcal{O} \equiv \frac{\Gamma_2}{(s - M_\pi^2)} = \frac{1}{\sqrt{2}} \left(A_1 \frac{1}{m} + A_2 \frac{\not{\omega}}{\omega{\cdot}p} \right) \gamma_5 \; , \tag{20}$$

and similarly for $\mathcal{O}'$ in terms of prime quantities. The components $A_{1,2}$ depend on $(x, \mathbf{R}_\perp^2)$, while $A'_{1,2}$ depend on $(x', \mathbf{R'}_\perp^2)$.

The kernel, $K^{\mu\nu}$, including the appropriate color factor, can be written as $K^{\mu\nu} = -g^{\mu\nu} \frac{4}{3} g^2 \mathcal{K}$ in the Feynman gauge, with

$$\mathcal{K} = \int \theta\left[\omega{\cdot}(k_1 - k_1')\right] \delta\left[(k_1 - k_1' + \omega\tau_1 - \omega\tau)^2\right] \frac{d\tau_1}{\tau_1 - i\epsilon} + \int \theta\left[\omega{\cdot}(k_1' - k_1)\right] \delta\left[(k_1' - k_1 + \omega\tau_1 - \omega\tau')^2\right] \frac{d\tau_1}{\tau_1 - i\epsilon} \; , \tag{21}$$

where τ and τ' are defined by

$$\tau = \frac{s - M_\pi^2}{2\,\omega{\cdot}p} \; , \quad \text{and} \quad \tau' = \frac{s' - M_\pi^2}{2\,\omega{\cdot}p} \; . \tag{22}$$

After integration over τ_1, we have

$$\mathcal{K} = \frac{\theta\left[\omega{\cdot}(k_1 - k_1')\right]}{-(k_1 - k_1')^2 + 2\tau\omega{\cdot}(k_1 - k_1')} + \frac{\theta\left[\omega{\cdot}(k_1' - k_1)\right]}{-(k_1' - k_1)^2 + 2\tau'\omega{\cdot}(k_1' - k_1)} \; . \tag{23}$$

Using the scalar products calculated in Appendix D of Ref. [28], one gets the following final expression for $\mathcal{K}$

$$\mathcal{K} = \frac{x'(x-1)\theta(x-x')}{\mathcal{K}_>} + \frac{x(x'-1)\theta(x'-x)}{\mathcal{K}_<} \; , \tag{24}$$

where,

$$\mathcal{K}_> = m^2(x-x')(x-x'-1) + \mathbf{R}_\perp{}^2 x'(x'-1) + \mathbf{R'}_\perp{}^2 x(x-1) - M_\pi^2 x'(x-1)(x-x') - 2x'(x-1)\mathbf{R}_\perp.\mathbf{R'}_\perp \; , \tag{25}$$

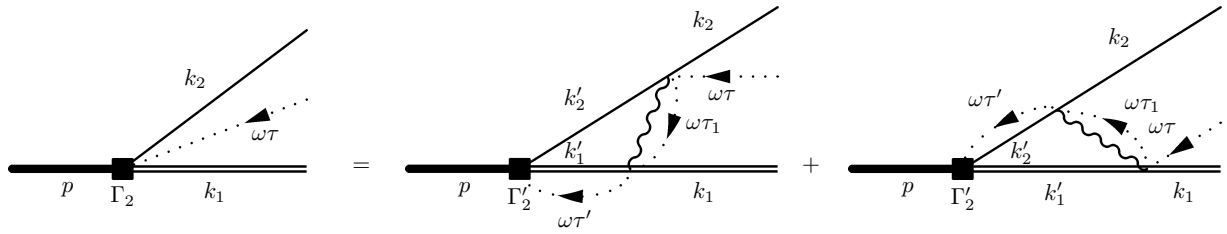

Fig. 2. Calculation of radiative corrections to the two-body wave function. In this figure, and in all subsequent figures, all particle lines are oriented from the left to the right.

and

$$\begin{aligned}\mathcal{K}_< = &= m^2(x-x')(x-x'-1) \\ &+\mathbf{R}_\perp{}^2 x'(x'-1) + \mathbf{R}'_\perp{}^2 x(x-1) \\ &+M_\pi^2 x(x'-1)(x-x') - 2x(x'-1)\mathbf{R}_\perp.\mathbf{R}'_\perp \ .\end{aligned} \tag{26}$$

The quark gluon coupling constant is denoted by g, with $g^2 = 4\pi\alpha_s$. In order to incorporate the correct short range properties of the quark-antiquark interaction from asymptotic freedom, we shall consider in the following a running coupling constant $\alpha_s(K^2)$, where K^2 is the off-shell momentum squared of the gluon. It is given by $K^2 = 1/\mathcal{K}$. We choose a simple parametrization which gives, in the large K^2 limit, the known behavior given by perturbative QCD. We take

$$\alpha_s(K^2) = \frac{\alpha_s^0}{1 + \frac{11-\frac{2}{3}n_f}{4\pi}\alpha_s^0 \mathrm{Log}\left[\frac{|K^2|+\Lambda_{QCD}^2}{\Lambda_{QCD}^2}\right]} \ . \tag{27}$$

At small K^2, it is given by the parameter α_s^0 which should be of the order of 1. We choose $n_f = 2$ and $\Lambda_{QCD} = 220$ MeV.

In order to extract the two components $A_{1,2}$, one should proceed as follows. We first multiply both sides of Eq. (17) by $u(k_2)$ on the left and $\bar{v}(k_1)$ on the right, and sum over polarization states. We then multiply both sides successively by γ_5 and $\not{\omega}\gamma_5$, and take the trace. We end up with the following system of two equations for the two unknowns $A_{1,2}$

$$\begin{aligned}&\mathrm{Tr}\Big[\gamma_5(\not{k}_2+m)\mathcal{O}(\not{k}_1-m)\Big] = \frac{1}{(s-M_\pi^2)(2\pi)^3} \\ &\times \int \mathrm{Tr}\Big[\gamma_5(\not{k}_2+m)A'_{\mu\nu}(\not{k}_1-m)\Big]K^{\mu\nu}\frac{\mathrm{d}^2\mathbf{R}'_\perp \mathrm{d}x'}{2x'(1-x')} \ ,\end{aligned} \tag{28}$$

and

$$\begin{aligned}&\mathrm{Tr}\Big[\not{\omega}\gamma_5(\not{k}_2+m)\mathcal{O}(\not{k}_1-m)\Big] = \frac{1}{(s-M_\pi^2)(2\pi)^3} \\ &\times \int \mathrm{Tr}\Big[\not{\omega}\gamma_5(\not{k}_2+m)A'_{\mu\nu}(\not{k}_1-m)\Big]K^{\mu\nu}\frac{\mathrm{d}^2\mathbf{R}'_\perp \mathrm{d}x'}{2x'(1-x')} \ ,\end{aligned} \tag{29}$$

with $A'_{\mu\nu}$ defined by

$$A'_{\mu\nu} = \gamma_\mu(\not{k}'_2+m)\mathcal{O}'(m-\not{k}'_1)\gamma_\nu \ . \tag{30}$$

In perturbation theory, we shall start from a non-relativistic pion wave function given by

$$\mathcal{O}^0 = \frac{1}{\sqrt{2}}\frac{A_1^0}{m}\gamma_5 \ , \tag{31}$$

where A_1^0 is calculated from (12) or (13) with $g_1 = g_1^0$ and $g_2 = 0$. The correction to the wave function coming from one gluon exchange is denoted by $\delta\mathcal{O}$ and given by

$$\delta\mathcal{O} = \frac{1}{\sqrt{2}}\left(\delta A_1 \frac{1}{m} + \delta A_2 \frac{\not{\omega}}{\omega.p}\right)\gamma_5 \ . \tag{32}$$

It is calculated from Eqs. (28,29) with the replacement $\mathcal{O} \to \delta\mathcal{O}$ in the l.h.-s. and $\mathcal{O}' \to \mathcal{O}'^0$ in the r.h.-s.. The total wave function is then given by

$$\mathcal{O} = \mathcal{O}^0 + \delta\mathcal{O} \ , \tag{33}$$

with

$$\begin{aligned}\delta A_1(x,\mathbf{R}_\perp^2) = &\frac{1}{(s-M^2)2\pi^2}\int \frac{\mathrm{d}^2\mathbf{R}'_\perp \mathrm{d}x'}{2x'(1-x')}\mathcal{K}A_1'^0\alpha_s(K^2) \\ &\times \frac{m^2(2x'^2-2x'+1)+\mathbf{R}'^2_\perp}{x'(1-x')} \ ,\end{aligned} \tag{34}$$

$$\begin{aligned}\delta A_2(x,\mathbf{R}_\perp^2) = &\frac{1}{(s-M^2)2\pi^2}\int \frac{\mathrm{d}^2\mathbf{R}'_\perp \mathrm{d}x'}{2x'(1-x')}\mathcal{K}A_1'^0\alpha_s(K^2) \\ &\frac{m^2(x-x')(x+x'-1)+\mathbf{R}_\perp^2 x'(1-x')-\mathbf{R}'^2_\perp x(1-x)}{x(1-x)x'(1-x')} \ .\end{aligned} \tag{35}$$

It is instructive to exhibit the behavior of these components at very high transverse momentum $|\mathbf{R}_\perp|$. From Eqs. (34,35), and using (24), it is easy to see that δA_1 is, in the absence of the running coupling constant, of the order of $1/\mathbf{R}_\perp^4$ while δA_2 is of the order of $1/\mathbf{R}_\perp^2$. The running of the coupling constant adds a factor $1/\mathrm{Log}\left[\frac{\mathbf{R}_\perp^2}{\Lambda_{QCD}^2}\right]$. At high transverse momentum, the relativistic component $A_2 = \delta A_2$ thus dominates. More precisely, we have, in this limit

$$\begin{aligned}A_2 \to A_2^\infty &= \frac{2}{3\pi^2}\frac{1}{\mathbf{R}_\perp^2 \mathrm{Log}\left[\frac{\mathbf{R}_\perp^2}{\Lambda_{QCD}^2}\right]}\int_0^1 \frac{\mathrm{d}x'}{2x'(1-x')}\frac{A_1'^0}{\bar{K}} \\ &\equiv \frac{1}{\mathbf{R}_\perp^2 \mathrm{Log}\left[\frac{\mathbf{R}_\perp^2}{\Lambda_{QCD}^2}\right]}\bar{A}_2^\infty(x) \ ,\end{aligned} \tag{36}$$

where $\bar{K} = x'/x$ for $x < x'$ and $\bar{K} = (1-x')/(1-x)$ for $x > x'$.

4 Physical observables

4.1 Decay constant

The pseudoscalar decay amplitude is given by the diagram in Fig. 3. According to the usual definition, the decay amplitude is $\Gamma_\mu = \langle 0|J^5_\mu|\pi\rangle$ where J^5_μ is the axial current. Since our formulation is explicitly covariant, we can decompose Γ_μ in terms of all four-vectors available in our system, i.e. the incoming meson momentum p and the arbitrary position, ω, of the light-front. We have therefore

$$\Gamma_\mu = F\ p_\mu + B\ \omega_\mu\ , \tag{37}$$

where F is the physical pion decay constant. In an exact calculation, B should be zero, while it is a priori non zero in any approximate calculation. It is a non physical, spurious, contribution which should be extracted from the full amplitude Γ_μ. Since $\omega^2 = 0$, the physical part of the pion decay constant can easily be obtained from

$$F = \frac{\Gamma\cdot\,\omega}{\omega\cdot p}\ . \tag{38}$$

Using the diagrammatic rules of CLFD [28], we can calculate Γ_μ from the graph indicated in Fig. 3. One gets, including color factors,

$$\Gamma_\mu = \sqrt{3}\int \frac{\mathrm{d}^3\mathbf{k_1}}{2\varepsilon_{k_1}}\frac{\mathrm{d}\tau}{\tau - i\epsilon}\delta(k_2^2 - m^2)\Theta(\omega\cdot k_2) \times \mathrm{Tr}\left[-\overline{\gamma_\mu\gamma_5}(\not{k}_2 + m)\Gamma_2(m - \not{k}_1)\right]\ , \tag{39}$$

with Γ_2 defined in (20) and where the notation $\overline{O}$ means as usual

$$\overline{O} = \gamma^0 O^\dagger \gamma^0\ . \tag{40}$$

After reduction of the scalar products, the decay constant is thus given by

$$F = \frac{2\sqrt{6}}{(2\pi)^3}\int \frac{\mathrm{d}^2\mathbf{R}_\perp \mathrm{d}x}{2x(1-x)}\left[A_1 + 2x(1-x)A_2\right]\ . \tag{41}$$

One can immediately notice that the pion decay constant given by (41) is divergent with the asymptotic relativistic component A_2^∞ given by (36). It diverges like Log Log $\mathbf{R}_\perp^2/\Lambda_{QCD}^2$. This divergence is extremely soft. It is in fact the expression of the well known divergence of radiative corrections in the process $q\bar{q} \to \gamma$. To get the physical contribution, we just subtract the minimal contribution arising when the integral on $|\mathbf{R}_\perp|$ is cut-off to Λ_C. The physical pion decay constant is thus

$$F^{phys} = F - F^\infty\ , \tag{42}$$

where

$$F^\infty = \frac{2\sqrt{6}}{4\pi^2}\frac{1}{\mathrm{Log\ Log}\left[\frac{\Lambda_C}{\Lambda_{QCD}}\right]}\int_0^1 \frac{dx}{2x(1-x)}\bar{A}_2^\infty(x)\ , \tag{43}$$

in the limit where Λ_C is very large, with $\bar{A}_2^\infty$ defined in Eq. (36).

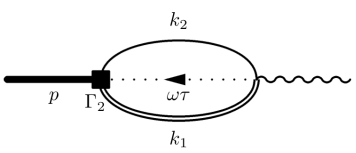

Fig. 3. Decay amplitude of the pion.

4.2 Electromagnetic form factor

The electromagnetic form factor is one of the most useful observable which can be used to probe the internal structure of a bound state. Moreover, from the electromagnetic form factor at very low momentum transfer, it is possible to determine the charge radius of the composite particle. This physical observable is therefore very powerful in order to constrain the phenomenological structure of the wave function both in the low and high momentum domains.

In the impulse approximation, the electromagnetic form factor is shown in Fig. 4. In CLFD, the general physical electromagnetic amplitude of a spinless system can be decomposed as [28]

$$J^\rho = \langle\pi(p')|e_q\,\bar{q}\gamma^\rho q|\pi(p)\rangle = e_\pi(p+p')^\rho\ F_\pi(Q^2) + \frac{\omega^\rho}{\omega\cdot p}B_1(Q^2)\ , \tag{44}$$

where e_q is the charge of the quark, while e_π is the charge of the pion. The physical form factor is denoted by $F_\pi(Q^2)$. In any exact calculation, $B_1(Q^2)$ should be zero. We choose for convenience a reference frame where $\omega\cdot q = 0$, with $q = p' - p$. This implies automatically that the form factors $F_\pi(Q^2)$ and $B_1(Q^2)$ depend on $Q^2 = -q^2$ only, since from homogeneity arguments their dependence on ω is of the form $\omega\cdot p/\omega\cdot p' \equiv 1$. The physical electromagnetic form factor $F_\pi(Q^2)$ can be simply extracted from J^ρ by

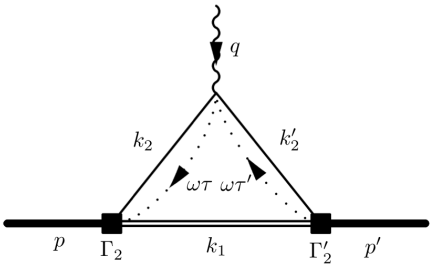

Fig. 4. Pion electromagnetic form factor in the impulse approximation. A similar contribution where the photon couples to the antiquark is not shown for simplicity.

contracting both sides of Eq. (44) with ω_ρ. One thus has

$$F_\pi(Q^2) = \frac{J\cdot\omega}{2\,\omega\cdot p}\ . \tag{45}$$

By using the diagrammatic rules of CLFD, we can write down the electromagnetic amplitude corresponding to Fig. 4 where the photon interacts with the quark. Assuming it is pointlike, one obtains:

$$\begin{aligned} F_\pi^{\gamma q}(Q^2) = e_q \int \frac{\mathrm{d}^3\mathbf{k_1}}{2\varepsilon_{k_1}} \frac{\mathrm{d}\tau}{\tau - i\epsilon}\delta(k_2^2 - m^2)\Theta(\omega\cdot k_2) \\ \times\ \frac{\mathrm{d}\tau'}{\tau' - i\epsilon}\delta(k_2'^2 - m^2)\Theta(\omega\cdot k_2') \\ \times\ \mathrm{Tr}\left[-\bar{\Gamma_2}'(\not{k}_2' + m)\frac{\not{\omega}}{2\omega\cdot p}(\not{k}_2 + m)\Gamma_2(m - \not{k}_1)\right], \end{aligned} \tag{46}$$

where Γ_2 is given in Eq. (20), and similarly for Γ_2' with prime quantities. After calculation of the trace, one gets

$$\begin{aligned} F_\pi^{\gamma q}(Q^2) = \frac{e_q}{(2\pi)^3}\int \frac{\mathrm{d}^2\mathbf{R}_\perp \mathrm{d}x}{2x(1-x)}\left[\frac{m^2 + \mathbf{R}_\perp^2 - x\mathbf{R}_\perp\cdot\mathbf{\Delta}}{x(1-x)m^2}A_1A_1'\right. \\ \left. + 2(A_1A_2' + A_1'A_2) + 4x(1-x)A_2A_2'\right]. \end{aligned} \tag{47}$$

The wave functions $A'_{1,2}$ depend on $(x', \mathbf{R}'^2_\perp)$, with $x' = x$ in the impulse approximation. If we define the four momentum transfer q by $q = (q_0, \mathbf{\Delta}, \mathbf{q}_\parallel)$, with $\mathbf{\Delta}\cdot\omega = 0$ and $\mathbf{q}_\parallel$ parallel to ω, we have $Q^2 = -q^2 \equiv \mathbf{\Delta}^2$, and thus $\mathbf{R}'_\perp = \mathbf{R}_\perp - x\mathbf{\Delta}$. The contribution from the coupling of the photon to the antiquark can be deduced from (47) by the interchange $x \iff (1-x)$, $\mathbf{R}_\perp \iff -\mathbf{R}_\perp$ and an overall change of sign.

One thus obtains the full contribution to the electromagnetic form factor of the pion

$$F_\pi(Q^2) = F_\pi^{\gamma q}(Q^2) + F_\pi^{\gamma\bar{q}}(Q^2)\ . \tag{48}$$

Note that this form factor, in the impulse approximation, is completely finite since it does not correspond to any radiative corrections at the γq vertex. The charge radius of the pion, $\langle r_\pi^2\rangle^{1/2}$, can be extracted from $F_\pi(Q^2)$ according to

$$\langle r_\pi^2\rangle = -6\frac{\mathrm{d}}{\mathrm{d}Q^2}F_\pi(Q^2)\Big|_{Q^2=0}\ . \tag{49}$$

In the very high Q^2 limit, it is now well accepted that the pion form factor behaves like $F_\pi(Q^2) \sim 1/Q^2$ (up to logarithmic corrections). This asymptotic behavior is fully determined by the one gluon exchange mechanism. This mechanism can either be considered explicitly in the hard scattering amplitude [13], or incorporated in the relativistic wave function of the meson. In the spirit of the relativistic constituent quark model, we adopt here the second strategy since it permits to investigate in a unique framework both low and high momentum scales. At asymptotically large Q^2, the form factor is dominated by the contribution from the relativistic A_2' component in Eq. (47) [28] calculated at $\mathbf{R}'^2_\perp \sim \mathbf{\Delta}^2$. We recover here naturally the asymptotic behavior of the pion electromagnetic form factor.

4.3 Transition form factor

The quantum numbers of the π transition amplitude, $\pi \to \gamma^*\gamma$, are similar to the ones of the deuteron electrodisintegration amplitude near threshold, as detailed in Ref. [28]. The exact physical amplitude, Γ_ρ, writes therefore

$$\Gamma_\rho = F_{\mu\rho}\ e^{\mu *}\ , \tag{50}$$

with the amplitude $F_{\mu\rho}$ given by

$$F_{\mu\rho} = \frac{1}{2}\varepsilon_{\rho\mu\nu\lambda}q^\nu P^\lambda F_{\pi\gamma}\ , \tag{51}$$

and where e^μ is the polarization vector of the final (on-shell) photon. The momenta P and q are defined by $P = p + p'$ and $q = p' - p$ with the kinematics indicated on Fig. 5. In any approximate calculation, the amplitude $F_{\mu\rho}$ depends on ω. It should be decomposed in terms of all possible tensor structures compatible with the quantum numbers of the transition, as we did above for the decay constant and the electromagnetic form factor. One thus has [28]

$$\begin{aligned} F_{\mu\rho} = \frac{1}{2}\varepsilon_{\rho\mu\nu\gamma}q^\nu P^\gamma F_{\pi\gamma} + \varepsilon_{\rho\mu\nu\gamma}q^\nu\omega^\gamma B_1 + \varepsilon_{\rho\mu\nu\gamma}p^\nu\omega^\gamma B_2 \\ + (V_\mu q_\rho + V_\rho q_\mu)B_3 + (V_\rho\omega_\rho + V_\rho\omega_\mu)B_4 \\ + \frac{1}{2m^2\omega\cdot p}(V_\mu p_\rho + V_\rho p_\mu)B_5\ , \end{aligned} \tag{52}$$

where $V_\mu = \varepsilon_{\mu\alpha\beta\gamma}\omega^\alpha q^\beta p^\gamma$. From Eq. (52), we can extract the physical form factor $F_{\pi\gamma}$ by the following contraction

$$F_{\pi\gamma} = \frac{i}{2Q^2(\omega\cdot p)}\varepsilon^{\mu\rho\nu\lambda}q_\nu\omega_\lambda F_{\mu\rho}\ . \tag{53}$$

For the transition form factor in the impulse approximation, the first relevant diagram, $F^a_{\mu\rho}$, is indicated in Fig. 5.

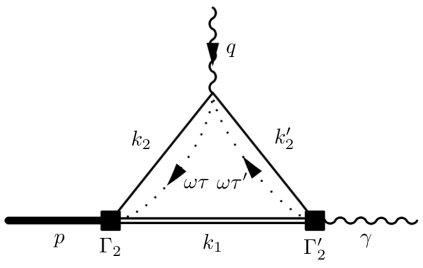

Fig. 5. Pion transition form factor in the impulse approximation. A similar contribution where the virtual photon, denoted by $\gamma*$, couples to the antiquark is not shown for simplicity.

By applying the diagrammatic rules of CLFD, we can derive the corresponding amplitude and get

$$F^a_{\mu\rho} = \sqrt{\frac{3}{2}}(e_u^2 - e_d^2)\int \frac{\mathrm{d}^3\mathbf{k_1}}{2\varepsilon_{k_1}}\frac{\mathrm{d}\tau}{\tau - i\epsilon}\delta(k_2^2 - m^2)\Theta(\omega{\cdot}k_2) \times \frac{\mathrm{d}\tau'}{\tau' - i\epsilon}\delta(k_2'^2 - m^2)\Theta(\omega{\cdot}k_2') \times \mathrm{Tr}\Big[-\overline{\gamma_\mu}(\not{k}_2' - \not{\omega}\tau' + m)\gamma_\rho(\not{k}_2 + m)\Gamma_2(m - \not{k}_1)\Big] \ . \quad (54)$$

The second contribution involving the coupling of the virtual photon to the antiquark can be calculated similarly. Other diagrams which should be taken into account at leading order either correspond to vacuum diagrams or are equal to zero for $\omega{\cdot}q = 0$. After calculation of the trace, the total amplitude for the transition form factor reads

$$F_{\pi\gamma}(Q^2) = \frac{4\sqrt{3}(e_u^2 - e_d^2)}{(2\pi)^3}\int \frac{\mathrm{d}^2\mathbf{R}_\perp \mathrm{d}x}{2x(1-x)} \times \frac{x}{m^2 + \mathbf{R}_\perp^2 - 2\mathbf{R}_\perp{\cdot}\boldsymbol{\Delta} + x^2Q^2} \times \left[A_1 + 2x(1-x)A_2 - \frac{\mathbf{R}_\perp{\cdot}\boldsymbol{\Delta}}{Q^2}(1-x)A_2\right] \ . \quad (55)$$

The transition form factor of the pion is completely finite thanks to the extra dependence on the transverse momentum as compared to the decay constant (41). The amplitude (54) includes a contact interaction associated to the elementary quark propagator between the virtual and real photons. It gives the factor $-\not{\omega}\tau'$ in this equation. Additional contributions from contact interactions are discussed below.

It is instructive to compare our result (55), with the one obtained in the asymtotic limit using the pion distribution amplitude [13]. This can be done by neglecting the mass term m^2 and the transverse momentum squared $\mathbf{R}_\perp{}^2$ in (55). We recover in this case the standard expression for the transition form factor and its $1/Q^2$ behavior. In our full calculation however, there is no need to regularize our expression in the $Q^2 \to 0$ limit in order to get the low momentum regime [15].

Comparing this result with the expression of the pion decay constant in (41), one may naively identify an "equivalent" distribution amplitude given by

$$\phi_\pi^{eq}(x) = \frac{1}{F}\frac{2\sqrt{6}}{(2\pi)^3)}\int \frac{d^2\mathbf{R}_\perp}{2x(1-x)}\left[A_1 + 2x(1-x)A_2\right] \ . \quad (56)$$

This "equivalent" distribution amplitude should be compared with the standard asymptotic one $\phi_\pi^{as} = 6x(1-x)$ normalized according to

$$\int \phi_\pi^{as}(x)dx = 1 \ . \quad (57)$$

This however can not be done safely since the limits $Q^2 \to \infty$ and $\mathbf{R}_\perp{}^2 \to \infty$ do not commute for the calculation of the transition form factor in (55). Indeed, one has to keep the full dependence of the transition form factor as a function of the transverse momentum in order to get a converged result in the limit $\mathbf{R}_\perp{}^2 \to \infty$. If we do the limit $Q^2 \to \infty$ by keeping $\mathbf{R}_\perp{}^2$ finite, the transition form factor is divergent, similarly to the calculation of the decay constant. This implies also that the "equivalent" distribution amplitude defined in (56) is divergent when δA_1 and δA_2 are calculated from a one gluon exchange process, as shown in Sec. 3.2.

4.4 Contact interactions

The contribution from one gluon exchange to the physical observables generates in LFD several terms involving contact interactions [27,28]. These ones originate from the singular nature of the LF Hamiltonian. According to the diagrammatic rules given in [28], one should add, to each fermion (anti-fermion) propagator between two elementary vertices, a contribution of the form $-\not{\omega}/2\omega{\cdot}k$ ($\not{\omega}/2\omega{\cdot}k$), where k is the momentum of the fermion. These contact interactions have been identified in [35] to part of the usual meson-exchange currents in the non-relativistic framework.

For the processes under consideration in this study, we have thus to consider extra contributions to the pion decay constant, electromagnetic and transition form factors. These are shown schematically in Figs. 6. The contact interaction is indicated by a dot on these figures. One can easily see that since the contact interaction is proportional to $\not{\omega}$, it does not contribute to the pion decay constant and electromagnetic form factor, according to Eqs. (38,45). Its contribution to the transition form factor is however very small, at most 1.5% for the highest measured momentum transfer. It is not included in the numerical results.

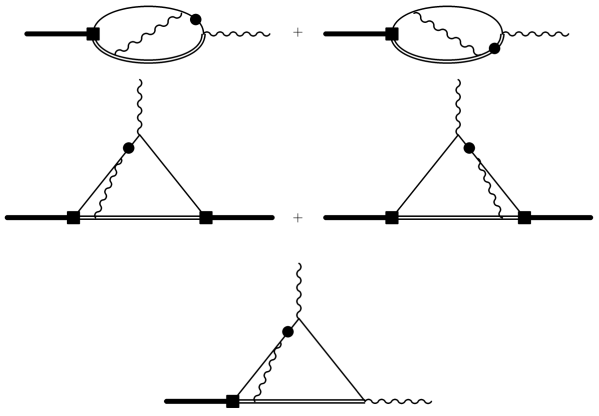

Fig. 6. Contribution from the contact interaction (full dot) to the pion decay constant, electromagnetic and transition form factors, from top to bottom respectively, in the impulse approximation.

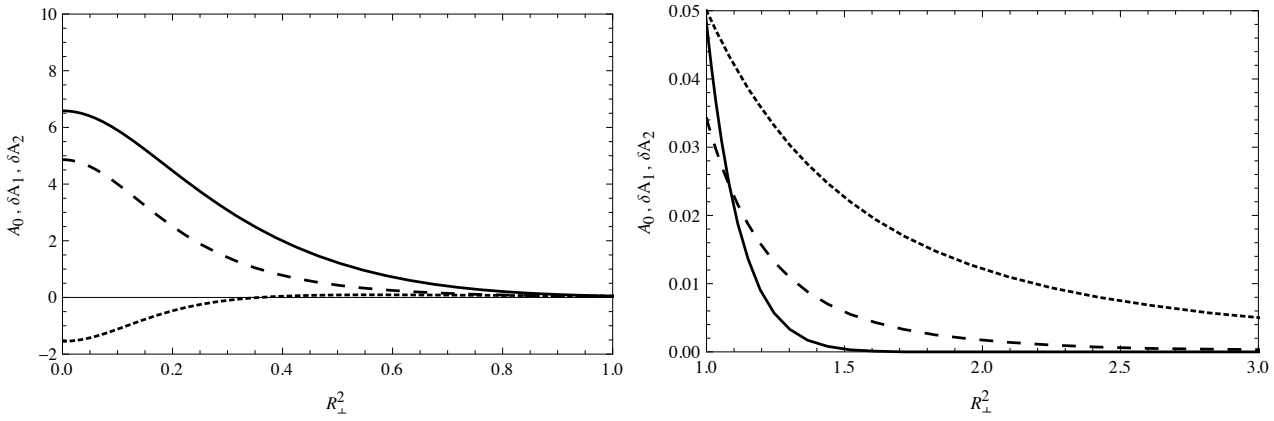

Fig. 7. The two components of the pion wave function calculated with a gaussian parametrization in the non-relativistic limit, both in the low (top curve) and high (bottom curve) momentum range. The solid line represents A_1^0 in (31) while the dashed (dotted) line represents δA_1 (δA_2) in (32). The calculation is done for $x = 0.5$.

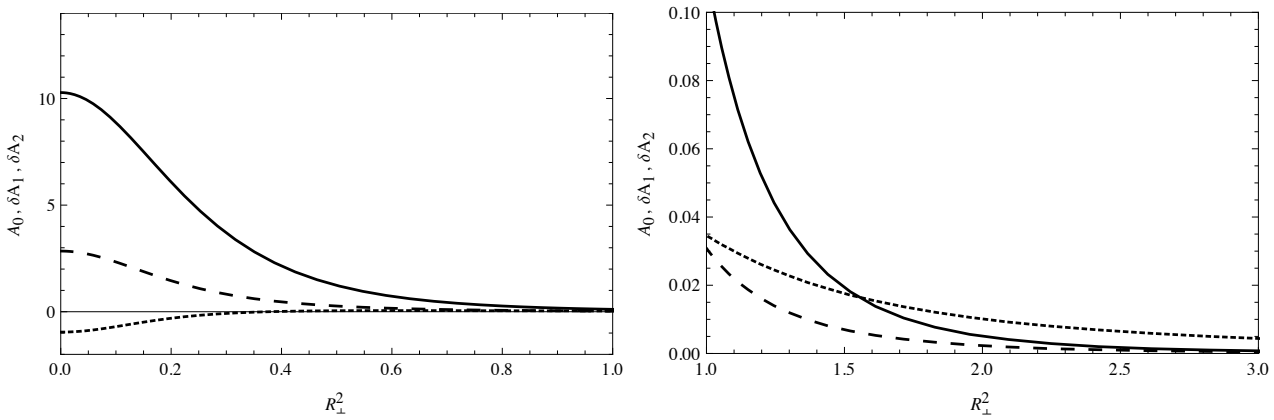

Fig. 8. Same as Fig. (7) but for the power-law parametrization.

5 Numerical results and discussion

Our phenomenological analysis has three independent parameters. The first one, β, gives the typical size of the non-relativistic wave function we start from in Eqs. (12,13). The second parameter is the quark (or antiquark) constituent mass m. The third one is the strong coupling constant in the low momentum region given by α_s^0 in Eq. (27). The values of these parameters are indicated in Table 1, for the two types of non-relativistic wave functions used in this study.

	β	m	α_s^0
Gaussienne w.f.	3.5	250 MeV	1.3
Power-law w.f.	3.72	250 MeV	0.35

Table 1. Parameter sets of the calculation.

These three parameters are fixed to get an overall good description of the pion decay constant, charge radius, electromagnetic and transition form factors. Since the pion decay constant and charge radius are known with a rather good accuracy, we fix two of the parameters to reproduce these quantities (within experimental errors), while the third one is fixed to get an overall good account of the pion electromagnetic and transition form factors at moderate Q^2.

We show in Figs. 7-8 the components A_1 and A_2 of the pion wave function for the two non-relativistic parametrizations used in this study, in both the low and high momentum range. In the low momentum range, the purely phenomenological component A_1^0 dominates. However, the contribution from one gluon exchange given by δA_1, is of the same order of magnitude for the gaussian parametrization, while it is a factor $2-3$ smaller for the power-law parametrization. This reflects directly the difference in the value of the coupling constant α_s^0. The relativistic component δA_2 is always smaller, but still sizeable.

In the high momentum domain, for $\mathbf{R}_\perp{}^2 > 1-2\ \mathrm{GeV}^2$, the relativistic component δA_2 dominates, as expected from its analytic behavior found in Sec. 3.2. We clearly see on these figures the interest to take into account the full structure of the pion wave function. It enables to describe,

in a unique framework, both the low and high momentum range.

F	Full	$\delta\mathcal{O}=0$	$\delta A_2=0$
Gaussian w.f.	131	92	140
Power-law w.f.	131	118	149

Table 2. Pion decay constant. All entries are in MeV.

$\langle r_\pi^2\rangle^{1/2}$	Full	$\delta\mathcal{O}=0$	$\delta A_2=0$
Gaussian w.f.	0.67	0.44	0.68
Power-law w.f.	0.67	0.54	0.68

Table 3. Pion charge radius. All entries are in fm.

Our predictions for the pion decay constant and charge radius are shown in Tables 2 and 3, respectively. The electromagnetic and transition from factors are shown in Figs. 9-10 for the two types of non-relativistic wave functions used in this study. Given the large experimental errors at large momentum transfer, we do not attempt in this study to get a best fit to all the data, but just to show that an overall agreement of all the available data is possible within our framework.

The pion electromagnetic form factor is shown in Figs. 9 together with the world-wide experimental data. Given the experimental errors which are large above 3 GeV^2, both parametrization (gaussian or power-law) give a rather good account of the data, in the whole kinematical domain available.

In order to settle the importance of the various components of the pion wave function, we also show in these figures the electromagnetic form factor calculated with $\delta A_2=0$ (dashed line). In the kinematical domain $Q^2<10$ GeV^2, the contribution of the component A_2 is rather small. This may be surprising given that A_2 dominates the wave function for ${\mathbf{R}_\perp}^2>2$ GeV^2, as shown in Figs. 7, 8. This indicates that the Q^2 domain where the asymptotic regime is dominant, i.e. where A_2 dominates in the calculation of the electromagnetic form factor according to (47), is very high. This is in full agreement with the early discussions in Refs. [36]. With our numerical parameters, it is above 100 GeV^2, much above the present experimental data. At moderate Q^2, both low and moderate momentum domain of A_2 dominate, and there is a partial cancellation between these contributions from the change in sign of δA_2 at about 0.5 GeV^2.

The dotted line on these figures shows the contribution of A_1^0 only. It is sizeably smaller than the full calculation. This originates directly from the importance of the δA_1 contribution to A_1 component, as shown on Figs. 7-8. Note that the complete calculations using the gaussian or power-law parametrizations are extremely similar, the only difference being in the value of δA_1 and δA_2. This may indicate that the most important feature, in this kinematical domain, is to have enough high momentum components in the pion wave function, either in the A_1 or in theA_2 components. It can come from the non-relativistic parametrization A_1^0 or from the one gluon exchange process giving rise to δA_1 and δA_2. Since the gaussian parametrization has very little high momentum components, this should be compensated by a larger α_s^0.

The corresponding results for the pion transition form factor are shown on Figs. 10. The qualitative, and to some extend also quantitative, features we get in this case are very similar to the ones detailed above for the electromagnetic form factor. At very high momentum transfer however, for $Q^2>15$ GeV^2, our results underestimate slightly the experimental data, with a better agreement when using a power-law wave function. There is no way to adjust our parameters to get a better agreement for the transition form factor without spoiling the good agreement we get for the electromagnteic form factor. We should however wait for more precise experimental data before drawing any definite conclusions.

6 Summary and discussion

We have investigated in this study the full relativistic structure of the pion in the framework of the constituent quark model. This structure involves two spin components, which, in turn, depends on two kinematical variables, like for instance the longitudinal momentum fraction and the square of the transverse momentum. This complete calculation has been made possible by the use of the explicitly covariant formulation of light-front dynamics [28]. Our phenomenological analysis has been compared with the full set of observables available at present: the pion decay constant, the charge radius, the electromagnetic and the transition form factors. These observables involve both low and high momentum scales.

Our wave function is constructed starting from a purely phenomenological wave function in the non relativistic limit. Relativistic kinematical corrections are thus included exactly using CLFD, while dynamical relativistic corrections are included by a one gluon exchange process. The latter generates the necessary relativistic high momentum components in the pion wave function.

From this full structure of the pion wave function, we have been able to obtain an overall very good agreement with all experimental data available, both in the low and high momentum domain. To get more physical insight into the relevant components of the wave function, it is however necessary to have more precise measurements of the pion electromagnetic form factor in the momentum range above $Q^2\simeq 5$ GeV^2. It is also necessary to confirm the recent Babar data for the pion transition form factor at very high momentum transfer (till about $Q^2\simeq 40$ GeV^2), with more precise data.

This analysis shows also the real flexibility of CLFD in describing few body systems in relativistic nuclear and particle physics. Its application to more fundamental cal-

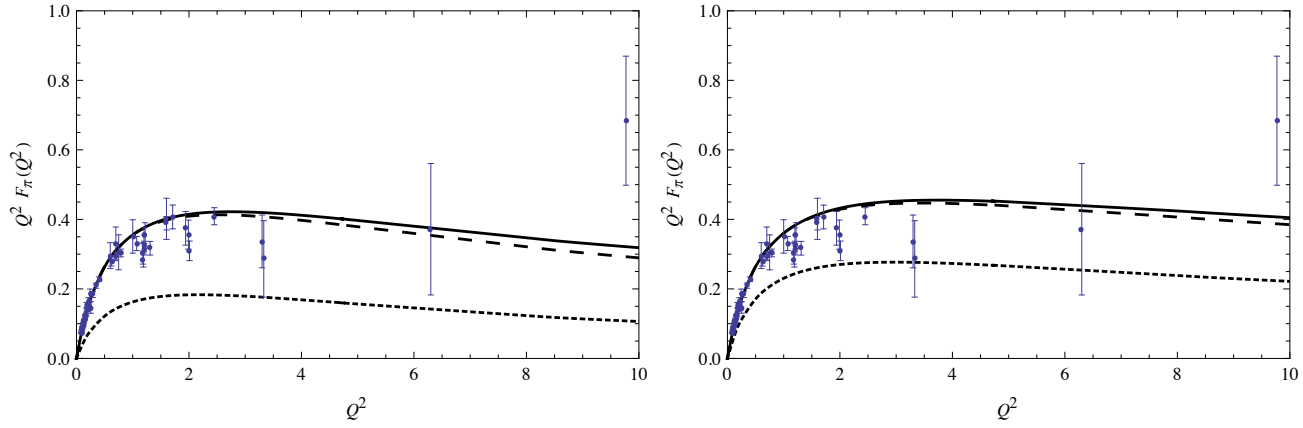

Fig. 9. Pion electromagnetic form factor calculated with a gaussian (left plot) and a power-law (right plot) wave functions in the non-relativistic limit. The solid line is the complete calculation, the dotted line is the calculation without any correction from one gluon exchange (i.e. with $\delta A_1 = \delta A_2 = 0$), while the dashed line corresponds to $\delta A_2 = 0$. The experimental data are from [4–11].

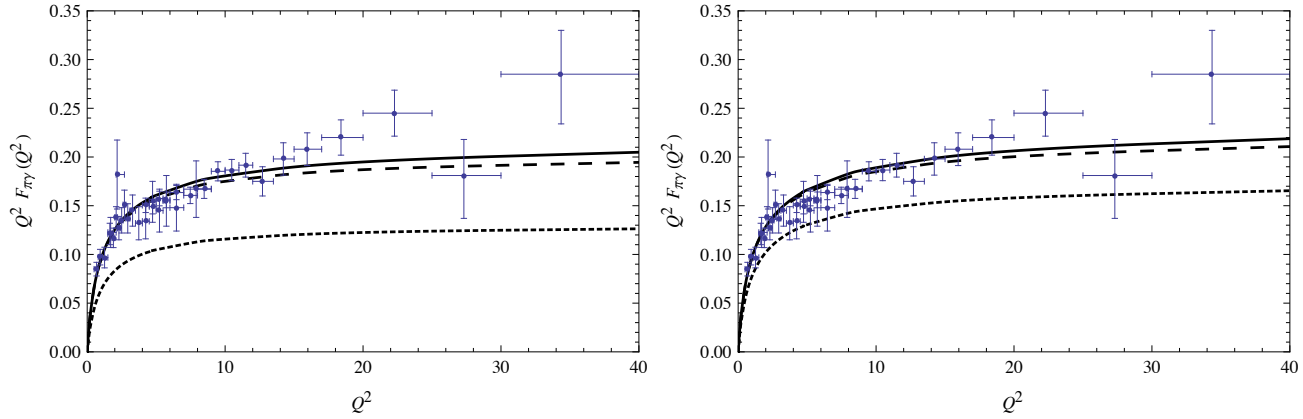

Fig. 10. Pion transition form factor calculated with a gaussian (left plot) and a power-law (right plot) wave functions in the non-relativistic limit. The solid line is the complete calculation, the dotted line is the calculation without any correction from one gluon exchange (i.e. with $\delta A_1 = \delta A_2 = 0$), while the dashed line corresponds to $\delta A_2 = 0$. The experimental data are from [1–3].

culations starting from first principles is also under way [37].

Acknowledgements

One of us (O.L.) would like to thank X.-H. Guo for useful and stimulating discussions. We also thank V. Karmanov for fruitful discussions and comments about this work.

References

1. B. Aubert *et al.*, Phys. Rev. **D80** (2009) 052002.
2. H.J. Behrend *et al.*, Z. Phys. **C49** (1991) 401.
3. J. Gronberg *et al.*, Phys. Rev. **D57** (1998) 33.
4. C.N. Braun *et al.*, Phys. Rev. **D8** (1973) 92.
5. C.J. Bebek *et al.*,Phys. Rev. **D17** (1978) 1693.
6. H. Ackermann *et al.*, Nucl. Phys. **B137** (1978) 294.
7. P. Brauel *et al.*, Z. Phys. **C3** (1979) 101.
8. S.R. Amendolia *et al.*, Phys. Lett. **B178** (1986) 435; Phys. Lett. *B277* (1986) 168.
9. J. Volmer *et al.*, Phys. Rev. Lett. **86** (2001) 1713.
10. T. Horn *et al.*, Phys. Rev. Lett. **97** (2006) 192001.
11. V. Tadevosyan *et al.*, Phys. Rev. **C75** (2007) 055205.
12. Review of Particle Physics, Phys. Lett. **B667** (2008) 1.
13. G.P. Lepage and S.J. Brodsky, Phys. Rev. **D22** (1980) 2157.
14. S. V. Mikhailov, N.G. Stefanis, Nucl. Phys. **B821** (2009) 291
15. S. Noguera and V. Vento, *" The pion transition form factor and the pion distribution amplitude"* arXiv: 1001.3075
16. A.P. Bakulev, S.V. Mikhailov, and N.G. Stefanis, Phys. Lett. **B508** (2001) 279.
17. H.N. Li and G. Sterman, Nucl. Phys. **B381** (1992) 129.
18. A. Schmedding and O.I. Yakovlev, Phys. Rev. **D62** (2000) 116002.
19. F.G. Cao, T. Huang and B.Q. Ma, Phys. Rev. **D 53** (1996) 6582.

20. I.V. Musatov and A.V. Radyushkin, Phys. Rev. **D56** (1997) 2713.
21. U. Raha and A. Aste, Phys. Rev. **D79** (2009) 034015.
22. R. Jakob and P. Kroll, Phys. Lett. **B 315** (1993) 463.
23. R. Jakob, P. Kroll, and M. Raulfs, J. Phys. **G22** (1996) 45.
24. T. Huang, X.G. Wu and X.H. Wu, Phys. Rev. **D70** (2004) 053007.
25. P. A. M. Dirac, Rev. Mod. Phys. **21**, 392 (1949).
26. V.A. Karmanov, Zh. Eksp. Teor. Fiz. **71**, 399 (1976); [transl.: Sov. Phys. JETP 44, 210 (1976)].
27. S. J. Brodsky, H.-C. Pauli, S. Pinsky, Phys. Reports **301** (1998) 299.
28. J. Carbonell, B. Desplanques, V.A. Karmanov and J.-F. Mathiot, Phys. Reports **300**, 215 (1998).
29. F. Bissey, J.-J. Dugne, J.-F. Mathiot, Eur. Phys. J. **C24** (2002) 101
30. P. Kroll and H. Raulfs, Phys. Lett. **B 387** (1996) 848.
31. V.M. Belyaev and M.B. Johnson, Phys. Rev. **D56** (1997) 1481.
32. F. Schlumpf, Phys. Rev. **D50** (1994) 6895.
33. S.J. Brodsky, T. Huang and P. Lepage, in *"Particles and Fields"*, A.Z. Capri and A.N. Kamal, Eds, Plenum Publishing Corporation, New-York 1983.
34. V.A. Karmanov, J.-F. Mathiot and A.V. Smirnov, Phys. Rev. **D77**, 085028 (2008).
35. V.A. Karmanov, B. Desplanques and J.-F. Mathiot, Nucl. Phys. **A589** (1995) 697
36. N. Isgur and C.H. Llewellyn Smith, Phys. Rev. Lett. **52** (1984) 1080; Phys. Lett. **B217** (1989) 535; Nucl. Phys. **B317** (1989) 526.
37. J.-F. Mathiot, *Field theory on the light front*, contribution to the conference "LC2010: relativistic hadronic and particle physics", Valencia (Spain), June 2010, to be published in Proceedings of Science.